NbTi Thin-Film SRF Cavities for Dark Matter Search

(Article begins on next page)

18 December 2024

NbTi Thin-Film SRF Cavities for Dark Matter Search

Giovanni Marconato , Cristian Pira , David Alesini, Domenico D'Agostino , Oscar Azzolini , Caterina Braggio, Roberta Caforio, Eduard Chyhyrynets, Alessandro D'Elia , Michela Fracasso , Umberto Gambardella, Vanessa Garcia, Claudio Gatti , Gianluca Ghigo , *Member, IEEE*, Daniele Di Gioacchino , Laura Gozzelino , Giorgio Keppel, Carlo Ligi , Giovanni Maccarrone , Nicola Pompeo , *Senior Member, IEEE*, Alessio Rettaroli , Alessandro Salmaso, Enrico Silva , *Senior Member, IEEE*, Fabrizio Stivanello, Simone Tocci , and Daniele Torsello , *Member, IEEE*

Abstract—The search for dark matter is now looking at axion-like particles (ALPs) as a very promising candidate to understand our universe. Within the framework of haloscope detectors for ALPs, we explore the performances of NbTi thin-film coatings on Cu resonating cavities to investigate the presence of axions in the range of 35–45-μeV mass. In this work, two different compositions of NbTi thin films are studied, and their performances in high magnetic field are presented. The chemical treatments and dc magnetron sputtering details of the preparation of three 9-GHz resonant cavities and a 7-GHz resonant cavity are shown along with the cavities' quality factor measurements at different applied magnetic fields.

Giovanni Marconato, Cristian Pira, Oscar Azzolini, Roberta Caforio, Eduard Chyhyrynets, Vanessa Garcia, Giorgio Keppel, Alessandro Salmaso, and Fabrizio Stivanello are with the INFN, Laboratori Nazionali di Legnaro, 35020 Padova, Italy (e-mail: giovanni.marconato@lnl.infn.it).

David Alesini, Alessandro D'Elia, Claudio Gatti, Daniele Di Gioacchino, Carlo Ligi, Giovanni Maccarrone, Alessio Rettaroli, and Simone Tocci are with the INFN, Laboratori Nazionali di Frascati, 00044 Frascati, Italy.

Domenico D'Agostino and Umberto Gambardella are with the Dipartimento di Fisica E.R. Caianiello, 84084 Fisciano, Italy, and also with the INFN, Sezione di Napoli, Gruppo collegato di Salerno, 84084 Fisciano, Italy.

Caterina Braggio is with the INFN, Sezione di Padova and Dipartimento di Fisica e Astronomia, University of Padova, 35131 Padova, Italy.

Michela Fracasso, Gianluca Ghigo, Laura Gozzelino, and Daniele Torsello are with the Department of Applied Science and Technology, Politecnico di Torino, 10129 Turin, Italy, and also with the INFN, Sezione di Torino, 10125 Turin, Italy.

Nicola Pompeo and Enrico Silva are with the Department of Industrial, Electronic and Mechanical Engineering, Università Roma Tre, 00146 Rome, Italy, and also with the INFN, Sezione di Roma Tre, 00146 Rome, Italy.

Color versions of one or more figures in this article are available at https://doi.org/10.1109/TASC.2024.3416541.

Digital Object Identifier 10.1109/TASC.2024.3416541

I. INTRODUCTION

A. Superconducting Haloscopes

AN OUTSTANDING result of modern cosmology is that a significant fraction of the universe is made of dark matter. However, the nature of such a component is still unknown, besides its gravitational interaction with ordinary baryonic matter. In the frame of quantum chromodynamics (QCD) of particle physics, the Peccei–Quinn mechanism offers a dynamic solution to the charge conjugation and parity transformation problem [1]. This solution involves the creation of a new particle called axion. There are also other types of axions called axion-like particles (ALPs), which are not necessarily related to QCD but are instead favored by other theories, namely, string theory.

Many projects explored the possibility to study the interaction of the cosmological axion with a strong magnetic field [2]. In fact, this interaction can cause the conversion of the ALP into a photon of frequency determined by its mass. Therefore, a possible detector for the axion in the range of masses 35–45 μeV could be a microwave resonant cavity cooled down at ultracryogenic temperature, to avoid the noise due to thermal photons, placed inside a strong magnetic field. This setup will be called haloscope hereafter. Since the mass of ALPs is unknown, many cavities have been fabricated to explore different frequencies within the range of interest. From previous studies, it is known that a high quality factor on the order of magnitude 10^6–10^7 is desirable [3]; therefore, the best choice is to look at superconducting materials that are notoriously used in particle accelerator resonant cavities with Q_0 on the order of 10^{10} even. The main difference with accelerating cavities is that haloscopes must operate and immerse in extremely high magnetic fields on the order of several tesla, so superconducting materials with high H_{c2} are required. In this work, hybrid superconducting–normal conducting haloscopes will be studied. In this configuration, the superconducting material is deposited as a thin film on the copper substrate using the dc magnetron sputtering (DCMS) technique. The cone-shaped ends of each cavity are not coated because these parts of the cavities are where most of the dissipation takes place since the magnetic field is not parallel to the cavity surface.

It was calculated that a superconductive film would dissipate more energy than the normal conductive copper surface due to flux vortex movement [4]. This represents one of the advantages of the use of thin-film-coated copper cavities compared with bulk superconducting cavities, where hybrid structures are not possible or at least more complex to fabricate.

B. NbTi in High-Magnetic-Field High-Frequency Regime

As previously mentioned, most of the energy dissipation in the superconducting part of the haloscopes is due to fluxon movement. Fluxons are quantized units of magnetic field flux that penetrate the type II superconducting material. The behavior of these fluxons in high-frequency fields can be described as a harmonic oscillator centered around the pinning center in the Gittleman–Rosenblum model using the following equation [5]:

$$m\ddot{x} + \eta\dot{x} + kx = J_{\mathrm{rf}}\,\Phi_0 \qquad (1)$$

where x is the fluxon displacement, m is its mass, η is the fluxon flow viscosity, kx is the pinning force, J_{rf} is the RF current in the superconductor, and Φ_0 is the flux quantization unit in superconductors. From these parameters, it is possible to define the depinning frequency $\nu_p = k/2\pi\eta$. The depinning frequency marks the border between two different regimes of operation: working with the radiation of frequency lower than ν_p, the fluxons wiggling around their pinning centers can be considered elastic and nondissipative. Working above ν_p means entering a resistive regime in which the fluxons do dissipate energy with their movement.

There are little data in the literature on η-values, particularly for coatings, so the choice of material was made by looking at superconductors used for magnet production. Among the most promising superconducting materials used for high-magnetic-field applications (Nb_3Sn, REBCO, etc.), NbTi was chosen, since it is one of the easiest to deposit as a thin film.

From previous studies [6], it is known that in NbTi alloys, the major contributor to the pinning of fluxons comes from α-Ti precipitates. It is, therefore, easy to figure out that the pinning force depends on the concentration of Ti, as well as on the magnetic field strength and working temperature. In Figs. 1 and 2, it can be seen that a maximum exists in the pinning force that depends on the titanium concentration and varies as the applied magnetic field increases and the working temperature decreases.

The first NbTi on Cu haloscope produced was a 9-GHz cavity coated by DCMS in 2019 [4], [8]. The goal of the present study is to improve the performance of this previous haloscope testing different NbTi compositions. We have also studied the effect of introducing a Nb barrier layer between the copper substrate and the NbTi layer to prevent diffusion at the interfaces. This barrier layer is commonly used in NbTi superconducting magnet production [9]. The vertical lines show the composition of the two NbTi alloys that will be presented in this study.

II. EXPERIMENTAL PROCEDURE

In this work, three copper 9-GHz microwave cavities (two half-cells each), one copper 7-GHz microwave cavity (two half-cells), one dielectric resonator (DR) sample, and two coplanar
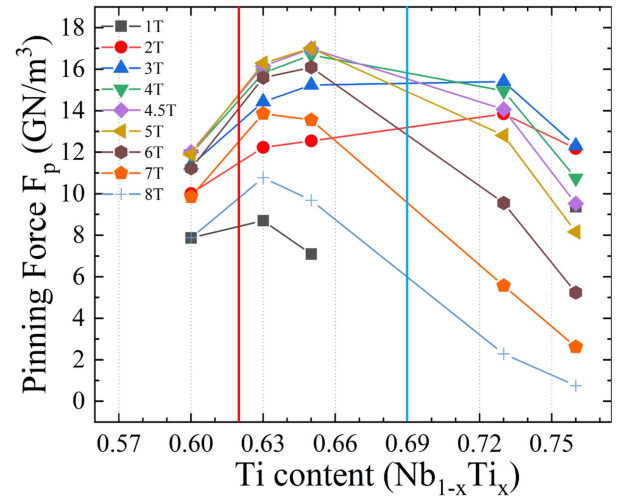
Fig. 1. Pinning force in function of the Ti content in the NbTi alloy at different applied magnetic fields at 4.2 K. The red and light blue vertical lines show the composition of the two NbTi alloys that will be presented in this study $Nb_{0.38}Ti_{0.62}$ and $Nb_{0.31}Ti_{0.69}$, respectively. Data adapted from [7].
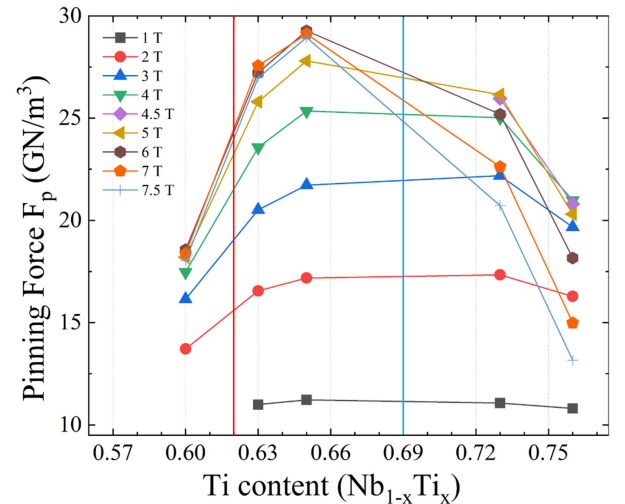
Fig. 2. Pinning force in function of the Ti content in the NbTi alloy at different applied magnetic fields at 1.8 K. The vertical lines show the composition of the two NbTi alloys that will be presented in this study $Nb_{0.38}Ti_{0.62}$ and $Nb_{0.31}Ti_{0.69}$, respectively. Data adapted from [7].

TABLE I
SUMMARY OF PRESENTED SAMPLES

$Nb_{0.38}Ti_{0.62}$ (low Ti content)	$Nb_{0.31}Ti_{0.69}$ (high Ti content)
9-GHz cavity	9-GHz cavity 9-GHz cavity (+ Nb barrier) 7-GHz cavity
One 20 x 20 mm quartz sample for DR	Two CPWR on 10 x 10 mm quartz samples

waveguide resonator (CPWR) samples were fabricated, coated with a superconducting NbTi thin film of two different compositions, and characterized. A summary of the samples prepared is presented in Table I.
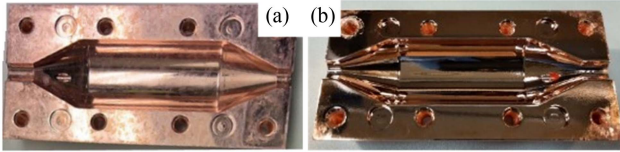
Fig. 3. 9-GHz cavity half-cell (a) before and (b) after polishing.

A. Cu Substrate Preparation

Copper semicell cavities were mechanically fabricated by CNC milling at INFN mechanical workshop starting from copper ingots. After mechanical fabrication, each semicell cavity was polished prior to the deposition process [see Fig. 3(a)]. The protocol used derived from ALPI linac quarter wave [10] and consisted in the following steps:

1) ultrasonic degreasing in GP17.40 soap at 40 °C for approximately 1 h;
2) ultrasonic cleaning in deionized water;
3) electropolishing in H_3PO_4 (85%): butanol (99,9%) at 3:2 volume ratio at room temperature with applied voltage 2–3 V for different times depending on the cavity shape and dimensions;
4) ultrasonic cleaning in deionized water, ethanol rinsing, and drying with nitrogen.

The two CPWRs were produced on commercial 10×10 mm quartz samples, polished by applying steps 1 and 2 of the copper cavity polishing protocol, while the DR sample was produced on commercial the 25×25 mm quartz substrate polished in the same way as the CPWR samples.

B. Coating Processes

The coatings were performed via DCMS by means of a 4-in NbTi planar target. The target–substrate distance was 9 cm. The sample holder was heated with IR lamps. The sputtering parameters used were: 24-h baking of the system at 600 °C, process temperature of 550 °C, process gas (Ar) pressure of 6×10^{-3} mbar, and 30-min sputtering time. The resulting NbTi layer showed a thickness of ∼2.5 μm (see Fig. 4). Two NbTi sputtering targets were chosen in this study: a 1-mm-thick $Nb_{0.38}Ti_{0.62}$ sheet (low Ti content) and a 5-mm-thick $Nb_{0.31}Ti_{0.69}$ commercial target (high Ti content).

The DR resonator sample and one copper 9-GHz resonator were coated using the low-Ti-content target. For these depositions, the process temperature was set to 500 °C instead of 550 °C.

Two copper 9-GHz cavities, one copper 7-GHz cavity, and two CPWRs were coated using the high-Ti-content target. On the CPWR sample, a waveguide resonator was subsequently patterned, as described in [11].

For the copper cavities, the two cone-shaped ends of each half-cell were masked during the sputtering process using two copper cones previously polished in SUBU-5 solution [12] and sputtered with Nb to prevent adhesion to the cells during the following sputtering process. The low-Ti-content 9-GHz cavity and
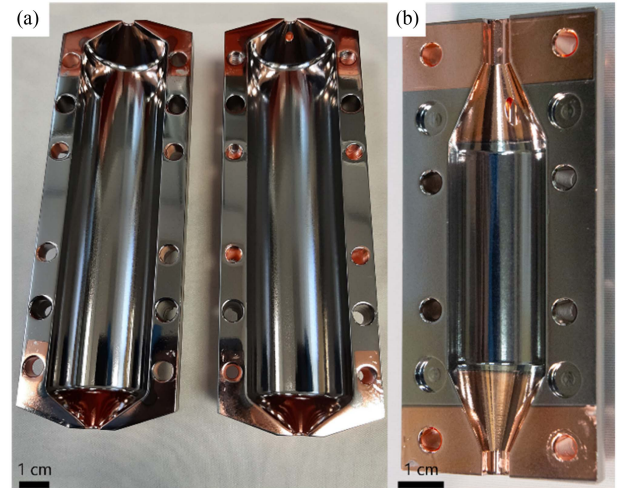

Fig. 4. (a) 7-GHz and (b) 9-GHz cavities half-cells after NbTi deposition via DCMS.

the high-Ti-content 7-GHz cavity were coated on a virgin polished copper substrate; meanwhile, for the two high-Ti-content 9-GHz cavities, two substrates, previously coated with NbTi and characterized, were used. The old coatings were removed chemically using a $HF:HBF_4$ solution [13]. The substrates were then polished using the four-point protocol described earlier.

C. Nb Barrier Layer

One of the two high-Ti-content 9-GHz cavities was coated inserting a 1-μm Nb barrier layer between the Cu substrate and the NbTi coating. The Nb barrier layer was coated ex situ using the following parameters: 36-h baking of the system at 550 °C, process temperature of 500 °C, process gas (Ar) pressure of 6×10^{-3} mbar, and 25-min sputtering time.

D. Characterizations

1) Planar Resonators: T_c of the planar resonators was measured by the inductive method on the quartz coated samples. For the DR sample characterization, the sample was placed on one of the bases of a dielectric-loaded cylindrical resonator and covered with a thin metal mask with a circular hole of diameter 17 mm. It is possible to extract the contribution of the sample to the Q_0 of the resonator and to the resonance frequency, as shown in [14], in function of the applied magnetic field. Similarly, it is possible to extract the properties of interest of the material itself [11] for the CPWR samples, by measuring the quality factor of the 2-D resonators previously patterned on the superconducting films [11].

2) Haloscopes: The haloscopes' Q_0 was measured cooling the devices inside a liquid helium bath cryostat and connecting them to a VNA. By analyzing the transmission and reflection scattering parameters of the haloscopes, Q_0 was extracted using a modified Lorentzian fit, as explained in [8]. The RF power sent via the VNA was kept below 1 mW.
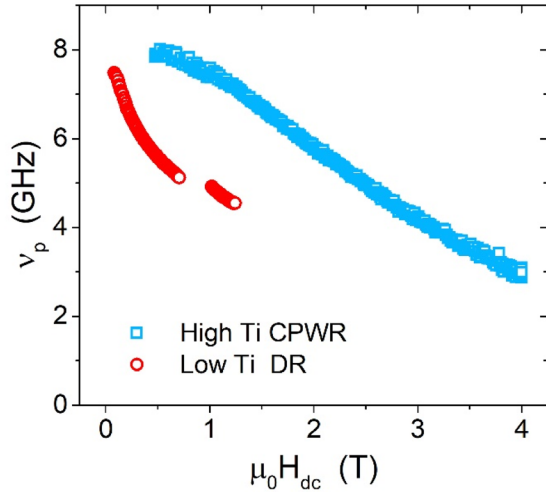
Fig. 5. Depinning frequency as a function of dc magnetic field. CPWR samples are the $Nb_{0.31}Ti_{0.69}$ samples, on which the resonator was patterned, while the DR sample is the $Nb_{0.38}Ti_{0.62}$ sample characterized at Roma Tre University.

Fig. 7. Quality factor of the 7-GHz haloscope in function of the applied magnetic field at different temperatures. The measurements were carried out at INFN Salerno apart from the single-point 15-mK measurement done at the University of Paris–Saclay with the use of a dilution refrigerator.
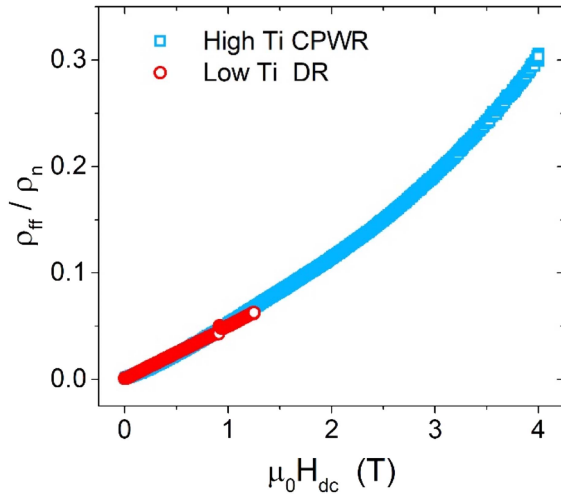

Fig. 6. Normalized flux flow resistivity as a function of dc magnetic field. As for Fig. 6, CPWR samples are the high-Ti-content samples with the resonator patterned on top, while the DR sample is the low-Ti-content sample characterized at Roma Tre University.
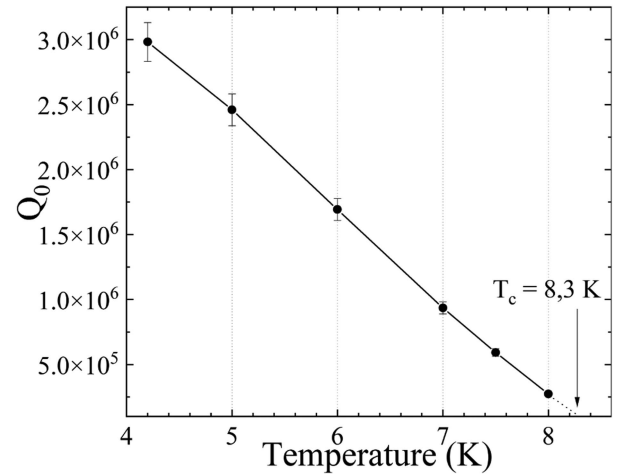
Fig. 8. Quality factor of the high-Ti-content 7-GHz cavity with no applied magnetic field in function of the temperature.

III. RESULTS

A. Material Characterization

The high-Ti-content quartz CPWR samples were characterized at the Politecnico di Torino, Turin, Italy, while the low-Ti-content sample was characterized at Roma Tre University, Rome, Italy, as previously described. Depinning frequency and flux flow resistivity of the superconducting material were extracted from quality factor measurements and plotted in function of the applied magnetic field (see Figs. 5 and 6). The lower maximum magnetic field in the DR measurement is due to the reduced capabilities of the normal conducting electromagnet used.

B. Cavity Characterization

Results of the 7-GHz cavity quality factor as a function of temperature and applied magnetic field are reported in Figs. 7 and 8.

Results of the first 9-GHz cavity quality factor as a function of the applied magnetic field are reported in Fig. 9.

In Fig. 9, high-Ti-content 9-GHz and high-Ti-content + Nb barrier layer 9-GHz cavities are also shown compared with the low-Ti-content 9-GHz cavity.

The characterization of 9-GHz cavities was carried out at INFN Frascati National Laboratories using a different magnet with lower capabilities with respect to the measurements done at INFN Salerno.

Fig. 9. Q_0 versus B for all the measured haloscopes at a temperature of 4.2 K. Data for the 9-GHz bare copper cavity from [8].

Fig. 10. R_s versus B for all the measured haloscopes at 4 K. The data for the 7-GHz haloscope are truncated in order to see clearly the comparison with 9-GHz haloscopes.

IV. DISCUSSION

The planar samples with low Ti ($Nb_{0.38}Ti_{0.62}$) content and high Ti ($Nb_{0.31}Ti_{0.69}$) content show very similar behavior as for the normalized flux flow resistivity (see Fig. 6), while the high-Ti-content samples show a smaller normal state resistivity (22 versus 54 $\mu\Omega\cdo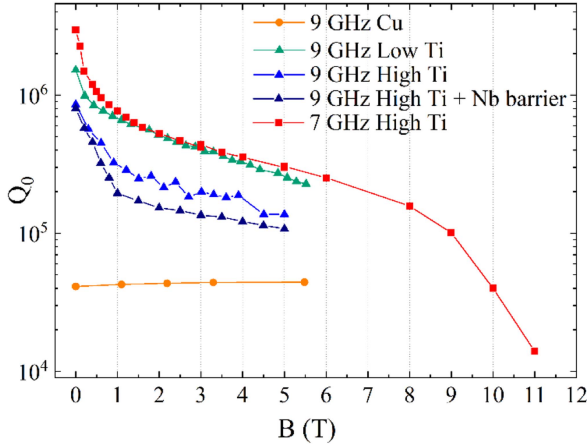t$cm) [11], which, together with the slightly higher depinning frequency (see Fig. 5), should lead to a better performance at the frequencies of interest (9 and 7 GHz).

As for the impact of the geometry on the quality factor of the haloscopes, it was estimated through Ansys software simulations of the 9-GHz haloscope that the maximum Q_0 achievable using the hybrid configuration should be 1.3×10^6 with no applied magnetic field. This value was calculated assuming no losses on the superconducting cylinder surface and considering $G_{\text{cones}} = 6270.11\ \Omega$ and $R_s^{\text{Cu}} = 4.9$ mΩ [4]. We expect a quite sharp step between the superconducting film and the not-coated copper ends that should not introduce significant losses, since the major source of dissipation should be fluxons' movement. It was not possible to characterize this interface due to the complex geometry of the samples.

Looking at the results for the 7-GHz cavity (see Fig. 7), we can notice that with rising temperature, a drop in the Q-factor is measured due to the progressive deprecation of the superconductive properties of NbTi approaching its T_c as expected. It is also important to notice that the drop of the performances of the device going to fields of $\sim$10 T (see Fig. 7) is due to NbTi reaching its H_{c2}.

Keeping the device at 4.2 K (liquid helium bath temperature) and progressively applying an external magnetic field parallel to the cylindrical surface of the cavity, it is possible to notice a reduction in the Q-factor most likely due to fluxon penetration and movement. The first fastest drop can be seen between 0 and 1 T, when the magnetic flux starts to penetrate in the material and forms the fluxons. Afterward, a small slope can be observed up to a field of 6 T that is still well below the theoretical H_{c2} of NbTi. Q_0 of 2×10^6 can be observed at no applied magnetic field and 4.2-K temperature, which is in accordance with simulations previously done for the 9-GHz hybrid geometry haloscope.
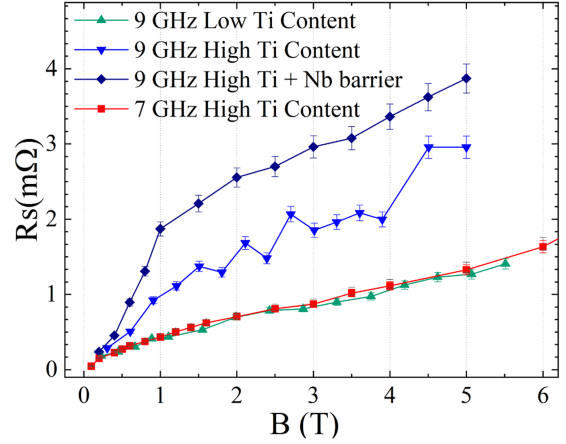
It is important to remember that these devices will have to work at millikelvin range temperatures because of the thermal noise reduction needed for axion detection. The reference value for the performance of this haloscope is the only available point at 15 mK and 2 T that gave $Q_0 \simeq 9 \times 10^5$. From the plot in Fig. 8, it is also possible to extract a rough estimate of the critical temperature of the high-Ti-content NbTi, yielding $T_c \simeq 8.3$ K. T_c limits the operating temperature, but since these haloscopes will be used at the millikelvin regime, it is not a limiting factor for the application. The seemingly linear dependence of the quality factor with temperature observed was also found for a different cavity and setup in [8]. Comparing the performances of low- and high-Ti-content 9-GHz cavities (see Fig. 9), although preserving a very similar shape to the low-Ti cavity's curve, the high-Ti coating is significantly less performing, in contrast with material characterization results done on planar resonators. Moreover, the introduction of a Nb barrier layer does not improve the results. This negligible effect of the Nb barrier layer shows that the thickness of the film is sufficiently bigger than the London penetration depth [11] on the whole cavity surface, making possible diffusion effects nonrelevant.

Looking at the comparison of the three cavities produced with the high-Ti-content NbTi coating (see Fig. 9), a significant increase in the quality factor can be seen at 7 GHz.

The surface resistance of each cavity was extracted calculating the G factor from simulations done in Ansys software (see Fig. 10). The two surface resistances of the 9-GHz low-Ti-content cavity and 7-GHz cavity align perfectly, while the other two haloscopes show a higher R_s and more pronounced slope. This may suggest that in addition to a frequency dependence, there might be a stronger contribution due to the substrate itself. In fact, the cavities that show higher Q_0 are the ones coated on pristine copper, while the two high-Ti-content 9-GHz cavities were deposited on a reused Cu substrate.

Moreover, the less-performing cavities showed defects on the copper surface not present in the other cavities, in particular on the cone-shaped edges, the area with the biggest contribution to the cavity losses with applied magnetic field (see Fig. 11).
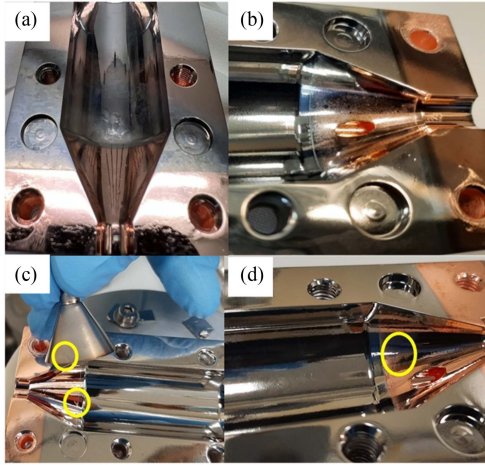
Fig. 11. Details of the high-Ti coating 9-GHz haloscope. (a) Presence of large grain boundaries. (b) Slight coating of the cone-shaped ends. (c) and (d) Scratches on the copper surface of the cones.

For example, partial coating of the copper cone-shaped ends was observed [see Fig. 11(b)]. This could introduce a fluxon movement dissipation contribution, explaining the rapid deprecation of the quality factor in function of the applied magnetic field. From the very long experience with cavities for particle accelerators, it is well known that surface imperfections are critical for the cavities' performances [15] and could, therefore, contribute to justify the low performances of the high-Ti-content 9-GHz cavities. A very big difference from elliptical cavity production procedure is the use of masks in contact with the cavity during the film deposition that could introduce scratches or imperfections, since after the deposition, it is not possible to further polish the samples. Further studies are needed to confirm the contribution of surface defects in the case of this hybrid cavity geometry.

V. CONCLUSION AND FUTURE DEVELOPMENTS

The possibility of producing high-performance haloscopes with hybrid geometry at 7 and 9 GHz with two different concentrations of NbTi coated via PVD was demonstrated. There is no clear evidence that either of the two NbTi compositions tested performs better than the other in high magnetic field. However, the surface quality of the copper substrate appears to strongly influence the quality factor, particularly at high magnetic fields. Therefore, surface treatments turn out to be critical as they already have demonstrated to be, for superconducting accelerator cavity technology. Further studies on the surface treatment and deposition procedure of NbTi on Cu will be carried out.

The contribution of the working frequency on the surface resistance requires further investigation. In this regard, a 3.9-GHz cavity has already been fabricated in collaboration with Fermilab, Batavia, IL, USA. A future improvement of the haloscopes' performances will also be the replacement of NbTi with Nb_3Sn thin films in order to push the quality factor to even higher values at higher magnetic fields. Studies on Nb_3Sn DCMS deposition are currently ongoing, looking at the best deposition parameters [16], [17].

REFERENCES

[1] R. D. Peccei, J. Solà, and C. Wetterich, "Adjusting the cosmological constant dynamically: Cosmons and a new force weaker than gravity," *Phys. Lett. B*, vol. 195, no. 2, pp. 183–190, Sep. 1987, doi: 10.1016/0370-2693(87)91191-9.

[2] Y. K. Semertzidis and S. Youn, "Axion dark matter: How to see it?," *Sci. Adv.*, vol. 8, no. 8, Feb. 2022, Art. no. eabm9928, doi: 10.1126/sci-adv.abm9928.

[3] D. Kim, J. Jeong, S. Youn, Y. Kim, and Y. K. Semertzidis, "Revisiting the detection rate for axion haloscopes," *J. Cosmol. Astroparticle Phys.*, vol. 2020, no. 3, Mar. 2020, Art. no. 66, doi: 10.1088/1475-7516/2020/03/066.

[4] D. Alesini et al., "Galactic axions search with a superconducting resonant cavity," *Phys. Rev. D*, vol. 99, no. 10, May 2019, Art. no. 101101, doi: 10.1103/PhysRevD.99.101101.

[5] S. Calatroni and R. Vaglio, "Surface resistance of superconductors in the presence of a DC magnetic field: Frequency and field intensity limits," *IEEE Trans. Appl. Supercond.*, vol. 27, no. 5, Aug. 2017, Art. no. 3500506, doi: 10.1109/TASC.2017.2691604.

[6] J. F. Li et al., "The microstructure of NbTi superconducting composite wire for ITER project," *Phys. C, Supercond.*, vol. 468, no. 15, pp. 1840–1842, Sep. 2008, doi: 10.1016/j.physc.2008.05.096.

[7] J. C. McKinnell, P. J. Lee, and D. C. Larbalestier, "The effect of titanium content on the pinning force in Nb44wt.%Ti to Nb62wt.%Ti," *IEEE Trans. Magn.*, vol. 25, no. 2, pp. 1930–1933, Mar. 1989, doi: 10.1109/20.92684.

[8] D. Di Gioacchino et al., "Microwave losses in a DC magnetic field in superconducting cavities for axion studies," *IEEE Trans. Appl. Supercond.*, vol. 29, no. 5, Aug. 2019, Art. no. 3500605, doi: 10.1109/TASC.2019.2897267.

[9] M. N. Wilson, "NbTi superconductors with low ac loss: A review," *Cryogenics*, vol. 48, no. 7, pp. 381–395, Jul. 2008, doi: 10.1016/j.cryogenics.2008.04.008.

[10] A. M. Porcellato et al., "Production, installation and test of Nb-sputtered QWRs for ALPI," *Pramana*, vol. 59, no. 5, pp. 871–880, Nov. 2002, doi: 10.1007/s12043-002-0101-9.

[11] G. Ghigo et al., "Vortex dynamics in NbTi films at high frequency and high DC magnetic fields," *Sci. Rep.*, vol. 13, no. 1, Jun. 2023, Art. no. 9315, doi: 10.1038/s41598-023-36473-x.

[12] C. Pira et al., "Impact of the Cu substrate surface preparation on Nb coatings for SRF," in *Proc. Int. Conf. RF Supercond.*, 2019, pp. 935–940.

[13] A. Salmaso, "Development of NbTi and Nb_3Sn thin films for innovative superconducting axion haloscopes," Master's thesis, Dept. Chem. Sci., Univ. Padova, Padua, Italy, 2022.

[14] A. Alimenti, K. Torokhtii, P. Vidal García, N. Pompeo, and E. Silva, "Design and test of a new dielectric-loaded resonator for the accurate characterization of conductive and dielectric materials," *Sensors*, vol. 23, no. 1, Jan. 2023, Art. no. 518, doi: 10.3390/s23010518.

[15] C. Antoine, "Materials and surface aspects in the development of SRF niobium cavities," French Alternative Energies and Atomic Energy Commission, Paris-Saclay, France, Tech. Rep. EuCARD-BOO-2012-001, 2012.

[16] D. Ford et al., "Study and improvement of liquid tin diffusion process to synthesize Nb_3Sn cylindrical targets," in *Proc. 21st Int. Conf. RF Supercond.*, 2023, pp. 868–871.

[17] D. Fonnesu et al., "Influence of the coating parameters on the T_c of Nb_3Sn thin films on copper deposited via DC magnetron sputtering," in *Proc. 21st Int. Conf. RF Supercond.*, 2023, pp. 92–95, doi: 10.18429/JACOW-SRF2023-MOPMB013.